Available online at www.sciencedirect.com
ScienceDirect
Journal of the European Ceramic Society 27 (2007) 3527–3538
www.elsevier.com/locate/jeurceramsoc

Synthetic resin-bonded transition-metal carbide–carbon hetero-modulus ceramics

Igor L. Shabalin *, Daniel L. Roach

Institute for Materials Research, The University of Salford, Greater Manchester M5 4WT, UK

Received 24 August 2006; received in revised form 5 February 2007; accepted 10 February 2007
Available online 6 April 2007

Abstract

Hetero-modulus ceramics (HMC) present an opportunity to combine a ceramic matrix having high Young's modulus with inclusions of a material having a considerably lower value of Young's modulus. The manufacturing method for the powder transition-metal carbide–graphite HMC with synthetic binder was studied. A statistical model for the cured-pressed carbide–carbon powder composition with resin binder was developed employing the statistical fractional factorial experimental design with the 2^{5-2} matrix type for several processing parameters. During the subsequent carbonisation of these compacts, the mutual influence between the carbide phase and the phenol–formaldehyde binder leads to the specific transformations in resin-bonded HMC. The pyrolysis reactions in the resin begin at lower temperatures and the products oxidise carbides with the formation of metal oxycarbides and oxides, so the behaviour of HMC depends strongly on the carbide content. The mass gain of carbonised compacts is compensated for by their swelling, so the bulk density in the wide range of contents does not vary after carbonisation. Possessing lower strength, the resin-bonded HMC have better thermal shock/fatigue resistance than materials hot-pressed at high temperatures.
© 2007 Elsevier Ltd. All rights reserved.

Keywords: Pressing; Composites; Carbides; Carbon; Hetero-modulus ceramics

1. Introduction

Hetero-modulus ceramics (HMC) present an opportunity to combine a ceramic matrix having high Young's modulus (300–600 GPa) with inclusions of a material having considerably lower values of Young's modulus (15–20 GPa). Subsequently, it becomes more effective to use brittle materials (carbides, nitrides, borides and oxides) in the most modern high-temperature engineering applications. The generally low thermal shock resistance of these brittle materials with high elastic moduli can be greatly improved by the addition of low-modulus graphite or graphite-like boron nitride. Similar materials, successfully applied in rocket and spacecraft design,[1,2] were referred to as "high-*E*–low-*E* composites" in the USA[3] and "hetero-modulus ceramics" in the USSR, Russia and Ukraine,[4–7] also known as "soft ceramics", with reference to the significant advantage of HMC, namely the remarkable machinability by conventional tools with a high grade of accuracy[4] that is normally unfeasible with conventional ceramics. The experience gained through the application of HMC was subsequently shifted from space and nuclear technologies to metallurgy and machinery, as HMC provided significant engineering opportunities.[4,5,10–12] The modification of HMC, refractory transition-metal carbide–carbon composites[5–12] are prospective materials for a number of high-temperature applications: as thermally stressed components of rocket engines, elements of thermal protection for re-entry flying apparatus, highly loaded brake-shoes in aviation and automotive engineering, diaphragms for casting metallurgical equipment, high-temperature lining and heating elements and others, including TiC–carbon composites, which (because of the relatively low *Z* of components) are real candidates for thermonuclear fusion reactors as plasma facing materials.[9]

High-temperature hot-pressing seems to be an established method for the manufacture of transition-metal carbide–graphite composite products.[10,11] However, there are a number of significant restrictions inherent to the fabrication of such compacts using high-temperature methods. As a result, the high financial cost of special tools for high-temperature hot-pressing as well as difficulties associated with the production of com-

* Corresponding author. Tel.: +44 161 295 3269; fax: +44 161 295 5147.
E-mail address: i.shabalin@salford.ac.uk (I.L. Shabalin).

0955-2219/$ – see front matter © 2007 Elsevier Ltd. All rights reserved.
doi:10.1016/j.jeurceramsoc.2007.02.198

Table 1
Physico-chemical characteristics of transition-metal refractory compound powders

Compound	Average particle size (μm)	Specific surface area ($m^2\ g^{-1}$)	Density ($g\ cm^{-3}$)		Lattice parameters (nm)	Chemical contents (wt%)						
			Pycnometric	XRD		Me	C[a]	O	N	B	W	(Fe + Co)[b]
TiC_{1-x}	4 ± 2	1.5	4.80	4.75	0.4328	78.0	19.1	0.5	0.4	–	1.5	0.4
ZrC_{1-x}	4 ± 2	1.6	6.45	6.44	0.4695	86.9	10.9	0.6	0.4	–	0.9	0.2
HfC_{1-x}	2 ± 1	2.5	12.10	12.52	0.4642	91.9[c]	6.8	0.7	0.5	–	0.8	0.1
ZrB_{2-x}[d]	2 ± 1	2.0	6.15	6.10	$a = 0.3172$; $b = 0.3525$	79.8	–	–	–	18.4	0.9	0.3

[a] Total carbon content.
[b] Sum total of iron and cobalt content.
[c] Sum total of hafnium and zirconium content.
[d] Used as an additive to ZrC_{1-x}.

pacts with complicated shapes and accurately controlled sizes, significantly hinder the wider application of carbide–carbon HMC. These restrictions make it desirable to develop a process for manufacturing HMC that requires lower temperatures and allows for the possibility of employing conventional tools for materials processing; a process that uses an appropriate binder, such as a synthetic carbonaceous resin, could help to avoid such a high level of expenses in energy, equipment and auxiliary materials. The advantages of the application of synthetic resins in the production of refractory materials are described in a recent review by Ewais,[13] but in practice only limited information about ceramics processing with synthetic binders, such as phenol–formaldehyde and phenol-furfural resins, is available in the literature. Such research in this field is presented only for refractory oxides[13–19] and non-metallic compounds.[20–22]

The goal of this work was to explore the feasibility of the application of synthetic resins as a binder for the fabrication of transition-metal carbide powder compositions with carbon and study the mutual influence and interaction between these refractory compounds and synthetic resins during the curing-pressing and heat treatment processing of carbide–carbon HMC over a range of temperatures and applied pressures. The study of these problems is also important for the development of a multi-temperature hot-pressing scheme for HMC production first proposed by Shabalin et al.[10] Such a scheme presents the opportunity of shape-forming of these materials through several stages of manufacture: at the beginning by low-temperature hot-pressing with the highest pressures that are possible by employing conventional pressing tools with application of temporary binders and/or lubricants, then by the moderate-temperature hot-pressing accompanied with the removal/transformation of the binder/lubricant for the subsequent formation of HMC and at the final stage of the scheme by high- or ultra-high-temperature hot-pressing employing special equipment.

2. Experimental

Fine powders of titanium, zirconium and hafnium carbides and zirconium diboride (as an additive to zirconium carbide) were used for the fabrication of HMC in this work. The powders of refractory compounds were produced by self-propagating high-temperature synthesis with subsequent milling in a WC–Co alloy lined rolling mill with the balls made from the same materials (Table 1). The powders of natural graphite marked YeUZ-M with lattice parameter $c = 0.678$ nm and mineral residue less than 0.1 wt% were taken as the low-modulus component. To compare the behaviour of carbon during the processing of HMC, different kinds of carbon black (CB) marked TG-10, PM-30 and PM-50 with mineral residue less than 0.15 wt% were also applied, where the number included in the brand of commercial CB approximately corresponds to its specific surface area measured in $m^2\ g^{-1}$.

Two kinds of synthetic resins were used as a carbonaceous binder for the carbide–carbon HMC:

- phenol–formaldehyde (Bakelite LBS-5), the solution of phenol–formaldehyde resol resin in ethanol with resin content of 50–55 wt%, free phenol content less than 8.0 wt% and water content less than 9.0 wt% and
- carbamide–formaldehyde–furan (Resin KF-90), the product of carbamide polycondensation with formaldehyde modified by furfuryl alcohol, with nitrogen content less than 9.0 wt%, free formaldehyde content less than 2.3 wt% and pH between 7.0 and 9.0.

The carbide–carbon powder compositions were prepared by mixing in a rolling mill with rubber-coated milling rods for 24 h. The carbonaceous binders LBS-5 or KF-90 with 3–5 wt% of oleinic acid as a surface-active compound (SAC) were diluted 2–4 times by ethanol or isopropanol and added to the powder compositions for the subsequent steps in the process. The higher level of dilution was used for compositions with higher carbon content. Dried in air at 50–70 °C for 1–2 h, the HMC were treated in a 35 mm diameter stainless steel die by uniaxial pressing with simultaneous heating by the electro-resistive method at defined values of processing parameters (temperature, pressure and time of treatment). The overview of the manufacturing process of synthetic resin-bonded HMC in general is presented in Fig. 1.

The mass and linear dimensions for compacted and carbonised samples of HMC were measured thoroughly before and after thermal treatment with at least 0.5% accuracy. The differential thermal analysis (DTA) was determined on a modified derivatograph in an argon atmosphere from room tempera-

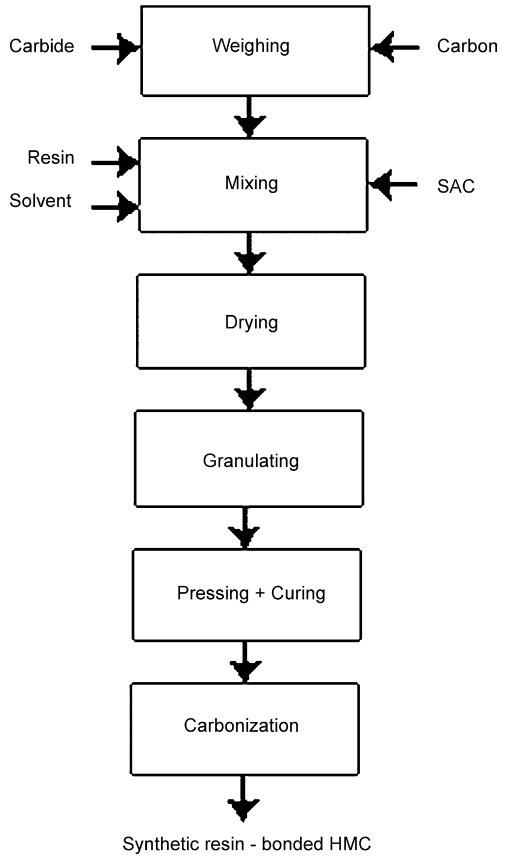

Fig. 1. Overview of the manufacturing process of synthetic resin-bonded HMC.

ture up to 1000 °C with heating rate 10–20 °C min^{-1}. For the thermogravimetric analysis (TGA), the samples (mass of about 0.3–0.6 g and sizes of 10 mm × 10 mm × 2 mm) were cut from the cured and pressed compacts; the surfaces of samples were preliminarily smoothed, polished and cleaned. The TGA was carried out in the isothermal regime with accumulation of gaseous products of carbonisation reactions, applying special equipment fitted with microbalance.[23] The pressure in the reaction chamber (volume of about 1 dm^3) was maintained in the range of 10–100 Pa. The heating up to the defined temperatures for the isothermal exposure proceeded at a rate of about 100 °C min^{-1}. Time of the exposure amounted to 2 h, though in practice the variation of mass for HMC samples was observed only during the first 20–40 min of each run. The X-ray diffraction (XRD) analysis of carbonised HMC was performed by employing the diffractometer DRON (Burevestnik, Russia) with Fe, Cu and Mo filtered radiation. The assessment of uniformity was accomplished by the microscopy analysis with an Epitype-2 (Carl Zeiss Jena, Germany) and an electron probe microanalysis (EPMA) with a Camebax MS 46 (France).

To test the carbonisation process of HMC with industrial equipment, a multi-chamber electro-graphite carbonisation gaseous furnace was used for the heat treatment of the TiC–C compacts with different carbide content. The TiC–C compacts containing 30 vol% phenol–formaldehyde binder LBS-5 were manufactured by uniaxial pressing at 250 °C and 70 MPa,

Table 2
The schedule of heat treatment in a multi-chamber electro-graphite carbonisation gaseous furnace used for the fabrication of synthetic resin-bonded TiC–C HMC

Current time of heat treatment (h)	Temperature (°C)	Average heating rate (°C h^{-1})
0	25	12.5
10	150	10
20	250	7
35	350	5
45	400	5
55	450	5
65	500	10
75	600	10
115	1000	10
125	1100	20
130	1200	0
135	1200	−20
140	1100	−16
200	150	–

exposed for 15 min. The samples of 35 mm in diameter and 15 ± 3 mm in height were set into 60 mm × 120 mm × 240 mm graphite capsule, which was closed with CB filling and graphite caps. The heat treatment of the experimental capsule with the TiC–C compacts was accomplished according to the regime shown in Table 2. Additionally, the experiments with substitution of TiC for the equimolar mixture TiO_2 with carbon were launched to evaluate the contribution of the redox processes to the formation of resin-bonded carbide–graphite HMC. The samples were prepared according to reaction:

$$TiO_2 + 3C \leftrightarrow TiC + 2CO \quad (1)$$

using identical methods and the same values of processing parameters. The only difference for the compacts containing $TiO_2 + 3C$ instead of TiC was the double reduction in weight of the $x(TiO_2 + 3C) + yC$ powder compositions compared with the $xTiC + yC$ compositions. This appeared to be necessary for the approximate conservation of the filler/binder ratio for the prepared materials.

For testing of the thermal shock/fatigue resistance, the samples of HMC were obtained by a curing-pressing procedure with subsequent carbonisation in the same industrial regime. The samples of carbonised compacts were machined into the shape of O-rings with outside diameter of 35 mm, height 15 mm and inside/outside diameters ratio $d/D = 0.5$. The samples were exposed to cyclic thermal shock loading by radial thermal flow from the arc-charge argon–nitrogen plasma jet of standard equipment.[24] Cycle times were controlled automatically by switching on and off with the shortest possible period (approximately 10 s). After thermal loading, the samples were tested with the universal testing machine ZOM 5/91 to determine the tensile strength rupture limit by the radial compression method.[25] These values were compared with the value for the high-temperature hot-pressed HMC before thermal loading.

3. Results and discussion

3.1. Pressing and curing of powder composition with synthetic binder

The pressing and curing procedure of carbide–graphite HMC with a synthetic resin as a binder is very important for the subsequent carbonisation process of the materials, so it was necessary to evaluate the effects of the main processing parameters (X_i) of the procedure on the general properties of the compacts (Y_k). These parameters, taken as independent variables (X_i) for the statistical fractional factorial experimental design with the 2^{5-2} matrix type, were:

- temperature of die (X_1 = 220–260 °C);
- applied pressure (X_2 = 40–80 MPa);
- phenol–formaldehyde binder content (X_3 = 20–45 vol%);
- carbide content in powder composition (X_4 = 45–75 vol%);
- time of curing-pressing treatment (X_5 = 15–25 min).

Within the framework of the developed statistical model, it was acceptable in the case of the volume content account in carbide–carbon HMC with synthetic binder to use the average value of 2.0 g cm^{-3} for the density of the carbon (graphite) phase.

The apparent bulk density of HMC compacts Y_1 (g cm^{-3}), is given as:

$$d_0 = \frac{M}{V} \tag{2}$$

where M is the mass of a compact, V the volume of a compact and the density of the so-called "unibinder" Y_2 (g cm^{-3}), which is expressed by the equation as follows:

$$d_b = \left(\frac{M - \sum_{i=1}^{i=n} M_i}{V - \sum_{i=1}^{i=n} V_i} \right) \tag{3}$$

where M_i is the mass of the ith powder component and V_i is the volume of the ith powder component; these were assigned as response functions (Y_k) in the experimental design for the above mentioned purposes.

The regression statistical analysis carried out at a 95% confidence level for the obtained experimental data shows that several of the coefficients in the equation:

$$Y_k = b_0 + \sum_{i=1}^{i=5} b_i X_i + \sum_{i,j=1}^{i,j=5} b_{ij} X_i X_j \tag{4}$$

possess much lower confidence, including all the coefficients that reflect the interconnections between the variables. In the coded form ($-1 \le X_i \le 1$), the expressions obtained for Y_1 and Y_2 are:

$$Y_1 = 2.50 + 0.068 X_2 + 0.097 X_4 \tag{5}$$

$$Y_2 = 0.564 + 0.257 X_3 + 0.111 X_5 \tag{6}$$

which can be converted to the conventional form:

$$d_0 = 1.91 + 3.4 \times 10^{-3} P + 6.5 \times 10^{-3} v_{MeC} \tag{7}$$

$$d_b = -0.548 + 0.021 v_b + 0.022 t \tag{8}$$

where P is the applied pressure (MPa), v_{MeC} the carbide content in powder composition (vol%), v_b the phenol–formaldehyde binder content (vol%) and t is the time of curing-pressing treatment (min).

Consideration of the obtained Eqs. (5)–(8) shows that, in the studied range (factorial space) of variables, both types of density are not affected by the temperature of the die X_1, although the applied pressure X_2 influences the bulk density of the material Y_1 alone. The density of the uni-binder Y_2, which is independent of the applied pressure X_2, represents not only the average density of the synthetic resin binder but also takes into account the macro- and microdefects (e.g. pores) at the boundaries between carbide and graphite micrograins as a characteristic of intergranular volume. Therefore, the independent behaviour of this property is essentially clear in this case. This is explained in terms of the elastic time effect ("green spring") and partial loss of binder through extrusion from gaps in pressing tools, which increase with a rise in applied pressure X_2. As a result of the above, the porosity of compacts could not be reduced by means of further pressure increase alone.

Applying some fundamental principles of powder technology,[26] it is possible to approximate the densities (Y_k) as a function of processing parameters $Y_k = f(X_i)$ in terms of a combination of two quasi-linear parts of the property–parameter plot, which are characterised by significantly different values of $\Delta Y_k / \Delta X_i$:

$$Y_k = \begin{cases} \left(\dfrac{\Delta Y_k}{\Delta X_i} \right)_1 X_i + Y_k(0), & -1 \le X_i \le X_{is} \\ \left(\dfrac{\Delta Y_k}{\Delta X_i} \right)_2 X_i + Y_k(X_{is}) + \delta, & X_{is} \le X_i \le 1 \end{cases} \tag{9}$$

where

$$\left(\frac{\Delta Y_k}{\Delta X_i} \right)_1 \approx \frac{Y_k(X_{is}) - Y_k(-1)}{X_{is} + 1} = A_{ki} = \text{const};$$

$$\left(\frac{\Delta Y_k}{\Delta X_i} \right)_2 \approx 0; \quad \delta \approx 0; \quad Y_k(0) = B_{ki}; \quad Y_k(X_{is}) = Y_{ks}$$

Hence, Eq. (9) can be simplified as follows:

$$Y_k = \begin{cases} A_{ki} X_i + B_{ki}, & -1 \le X_i \le X_{is} \\ Y_{ks}, & X_{is} \le X_i \le 1 \end{cases} \tag{10}$$

where X_{is} is the so-called point of "saturation", which divides the region of variable values into two parts, and Y_{ks}, respectively, the "saturation" value of the property corresponding to the constant (approximated) value of Y_k in the second part of plot (Fig. 2).

The dependencies of bulk density Y_1 on carbide content X_4, varying from 0 to 90 vol% for the different types of carbide–carbon HMC, are shown in Fig. 3. For the materials with $v_{MeC} < 45$ vol%, the negative deviation from linearity is explained by a significant increase of the specific surface area of the powder mixture due to the increase of carbon volume content. The introduction of similar refractory compounds to carbide–graphite HMC does not upset the linear form of the

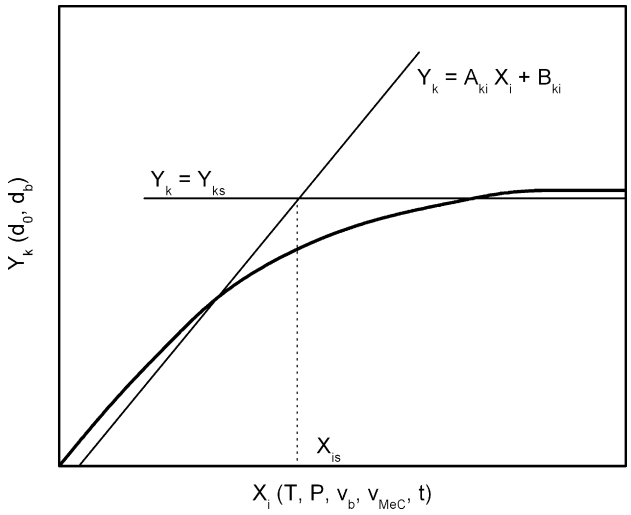

Fig. 2. Graphical interpretation of the model of the property–parameter plot $Y_k = f(X_i)$ for the carbide–carbon compacts formed with synthetic resin binder.

density–content plot, as was shown experimentally for the addition of zirconium diboride to zirconium carbide compositions (Fig. 4). The application of different kinds of CB as a carbon component in compositions with carbides leads to the necessity of increasing the binder content for the fabrication of compacts with the same values of apparent bulk density. For a larger specific surface area, one would expect to use a proportionally increased amount of synthetic binder (Fig. 5). Within the framework of the developed model for carbide–carbon compacts with binder, this behaviour becomes clear and can be interpreted as a shift of X_{3s} to a region of higher values of X_3.

3.2. Pyrolysis of synthetic binder and concurrent processes

The variation of mass due to pyrolysis of a synthetic binder in the carbide–carbon HMC, taking into account the coke yield

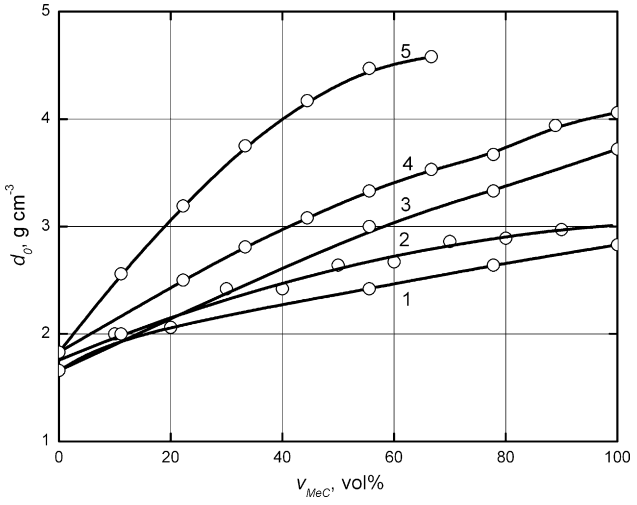

Fig. 3. The apparent bulk density of compacts vs. the volume content of powder carbide for transition-metal carbide–graphite compositions with 30 vol% of synthetic resin binders cured and pressed at 250 °C and 60 MPa: (1) TiC–C (Resin KF-90); (2) TiC–C (Bakelite LBS-5); (3) ZrC–C (Resin KF-90); (4) ZrC–C (Bakelite LBS-5); (5) HfC–C (Bakelite LBS-5).

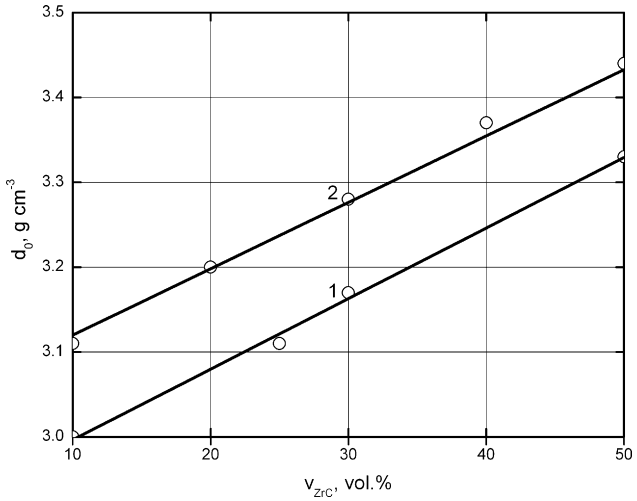

Fig. 4. The apparent bulk density of compacts vs. the volume content of carbide for zirconium carbide–graphite compositions with additives of zirconium diboride (30 vol% of Bakelite LBS-5) cured and pressed at 250 °C and 60 MPa: (1) ZrC–0–40 vol% ZrB_2–50 vol% C; (2) ZrC–10–50 vol% ZrB_2–40 vol% C.

of binder in percentage, κ, is given by:

$$\left(\frac{\Delta M}{M}\right)_{\kappa} = \frac{cv_{\mathrm{b}}d'_{\mathrm{b}}(\kappa - 100) \times 100\%}{(100 - v_{\mathrm{b}})\left(v_{\mathrm{MeC}}d_{\mathrm{MeC}} + v_{\mathrm{C}}d_{\mathrm{C}} + \sum_{i=1}^{i=n} v_i d_i\right) + 100cv_{\mathrm{b}}d'_{\mathrm{b}}} \quad (11)$$

where c denotes the degree of solvent dilution, d'_{b} the binder content in solution (g cm^{-3}), v_{MeC} and v_{C} the carbide and carbon content of the powder composition (vol%), respectively, d_{MeC} and d_{C} the densities of each of the carbide and carbon phases (g cm^{-3}) and v_i and d_i are the content of powder composition

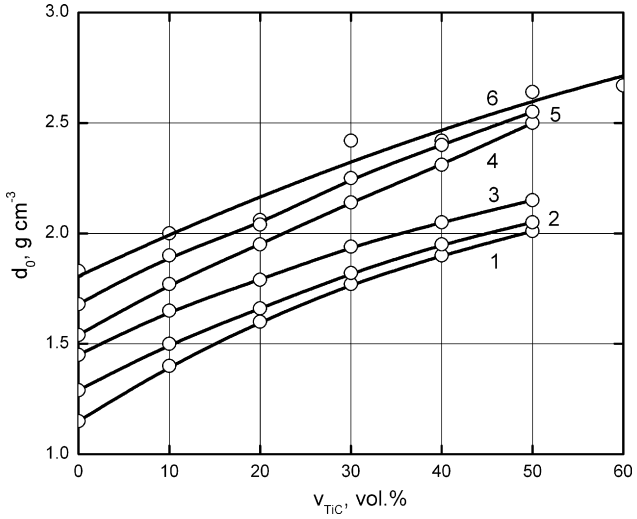

Fig. 5. The apparent bulk density of compacts vs. the volume content of carbide for titanium carbide–carbon compositions with different kinds of carbon and binder contents pressed and cured at 250 °C and 60 MPa (volume contents of Bakelite LBS-5 are given in parentheses): (1) CB PM-50 (30%); (2) CB PM-50 (35%); (3) CB PM-50 (40%); (4) CB PM-30 (30 and 35%); (5) CB TG-10 (30%); (6) Graphite YeUZ-M (30%).

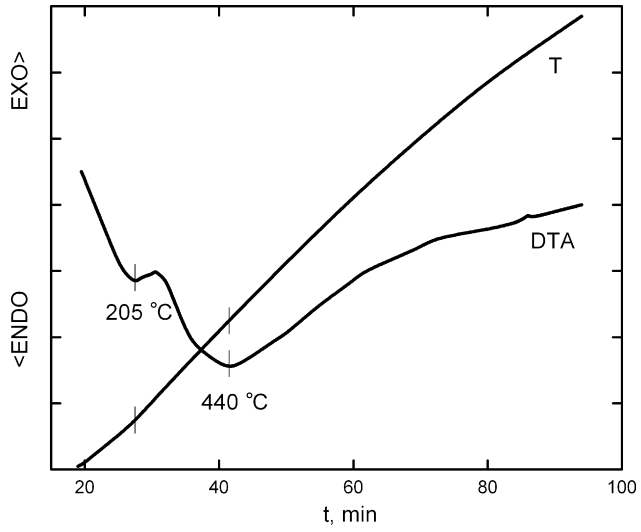

Fig. 6. The derivatogram of the 90 vol% TiC–10 vol% C (graphite) composition with 30 vol% of Bakelite LBS-5 binder in an argon atmosphere.

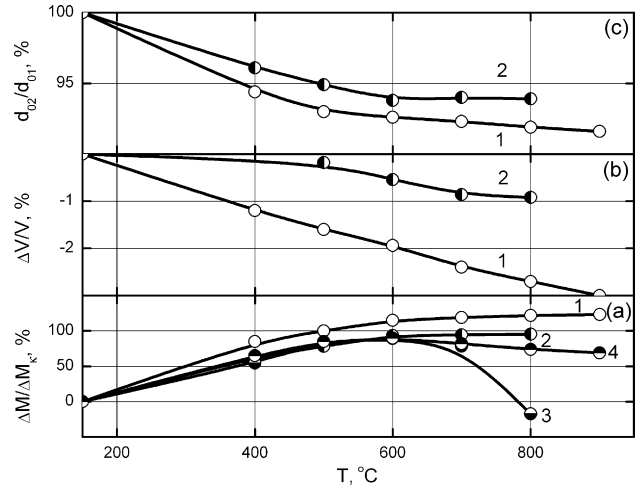

Fig. 7. The relative variations of mass (a), volume (b) and apparent bulk density (c) vs. the temperature of vacuum carbonisation with accumulation of pyrolysis products for the metal carbide–graphite compacts with 30 vol% of Bakelite LBS-5 binder: (1) 10 vol% TiC–90 vol% C; (2) 10 vol% ZrC–90 vol% C; (3) 90 vol% ZrC–10 vol% C; (4) 30 vol% ZrC–30 vol% ZrB_2–40 vol% C.

(vol%) and the density (g cm^{-3}) of the *i*th modifying additive, respectively. The increase of carbon content in the composition after similar heat treatment can be shown to be:

$$\Delta v_C(\%) = \frac{c v_b d'_b \kappa \left(v_{MeC} + \sum_{i=1}^{i=n} v_i \right)}{c v_b d'_b \kappa + 100 d_C (100 - v_b)} \quad (12)$$

The accepted scheme of the pyrolysis (thermal destruction) of phenol–formaldehyde resins during heat treatment from 150 to 1000 °C includes[27–32]:

- at 150–350 °C, the dehydration from post-curing reactions and the increase of the degree of cross-linking;
- at 350–400 °C, the dehydration and formation of diphenyl ether structures by the reaction with hydroxyl and methylene groups and thermal branching (fragmentation) of the polymer structure to yield lower molecular weight species;
- at 400–600 °C, the liberation of gaseous by-products: carbon monoxide formed due to the decomposition of ether linkages, methane formed from the cleavage of methylene bridges as well as carbon dioxide, water vapour and hydrogen; the formation and isomerisation of heterocycles as well as the formation and subsequent structurisation of carbocycles stabilised by aliphatic bridges;
- at 600–700 °C, the condensation of aromatic ribbon molecules and destruction of 3D polymers, accompanied by the liberation of hydrogen;
- above 700 °C, the continuous dehydrogenation and aromatisation of the whole carbonaceous structure.

With reference to the only communication on the problem by Lukina et al.,[33] it is clear that the catalytic activity of transition-metal carbides, especially in the form of fine powders with developed surface areas, effectively transform the process of thermal degradation of phenol–formaldehyde resin.

A typical derivatogram of the carbide–graphite HMC with phenol–formaldehyde binder is shown in Fig. 6. The samples of material showed an endothermal peak at about 205 ± 5 °C, which corresponds to the dehydration reactions inherent to the post-curing cross-linking processes of Bakelite LBS-5, as the curing-pressing of resin is characterised by a deficiency of time for the completion of polycondensation reactions. Another feature of the DTA plot of the phenol–formaldehyde resin-bonded MeC–C HMC is the existence of the broad endothermal range, starting at about 270 °C and with a maximum at 440 ± 10 °C. Most likely, this range reflects the destruction processes connected with the split of methylene bridges and ether linkages of polymer, accompanied by intensive liberation of gaseous by-products. It was observed that the analogous processes in pure phenol resins proceed at higher temperatures,[16] though there are some publications that give just the opposite signs to the DTA peaks obtained from pyrolysis of phenol–formaldehyde resins.[34] Taking into account the fact that the graphite filler does not cause phenol resin decomposition,[30] this observation confirms the influence of carbide as a catalyst of pyrolitic reactions, but no reproducible effects on the DTA plot correlated with the carbide content in the powder composition or any other processing parameters in this study.

However, during the pyrolysis in the resin-bonded HMC, the back influence of the binder, particularly the products of binder destruction, on the carbide phase of HMC was also detected. This leads to the partial oxidation of the carbide, which was sometimes visible in the external appearance of the samples after carbonisation heat treatment. The combined TGA, dilatometric (shrinkage) and densitometric measurement data for different materials carbonised with the accumulation of gaseous products of reactions at pressure of 10–100 Pa are shown in Fig. 7. The TGA data conformed to the value of ΔM_κ, which was calculated according to Eq. (11). For those calculations, the magnitude of the coke yield for Bakelite LBS-5, $\kappa = 50.5 \pm 0.5\%$ was determined experimentally in free-carbide graphite compositions by slow heating of samples (<0.5 °C min^{-1}) up to

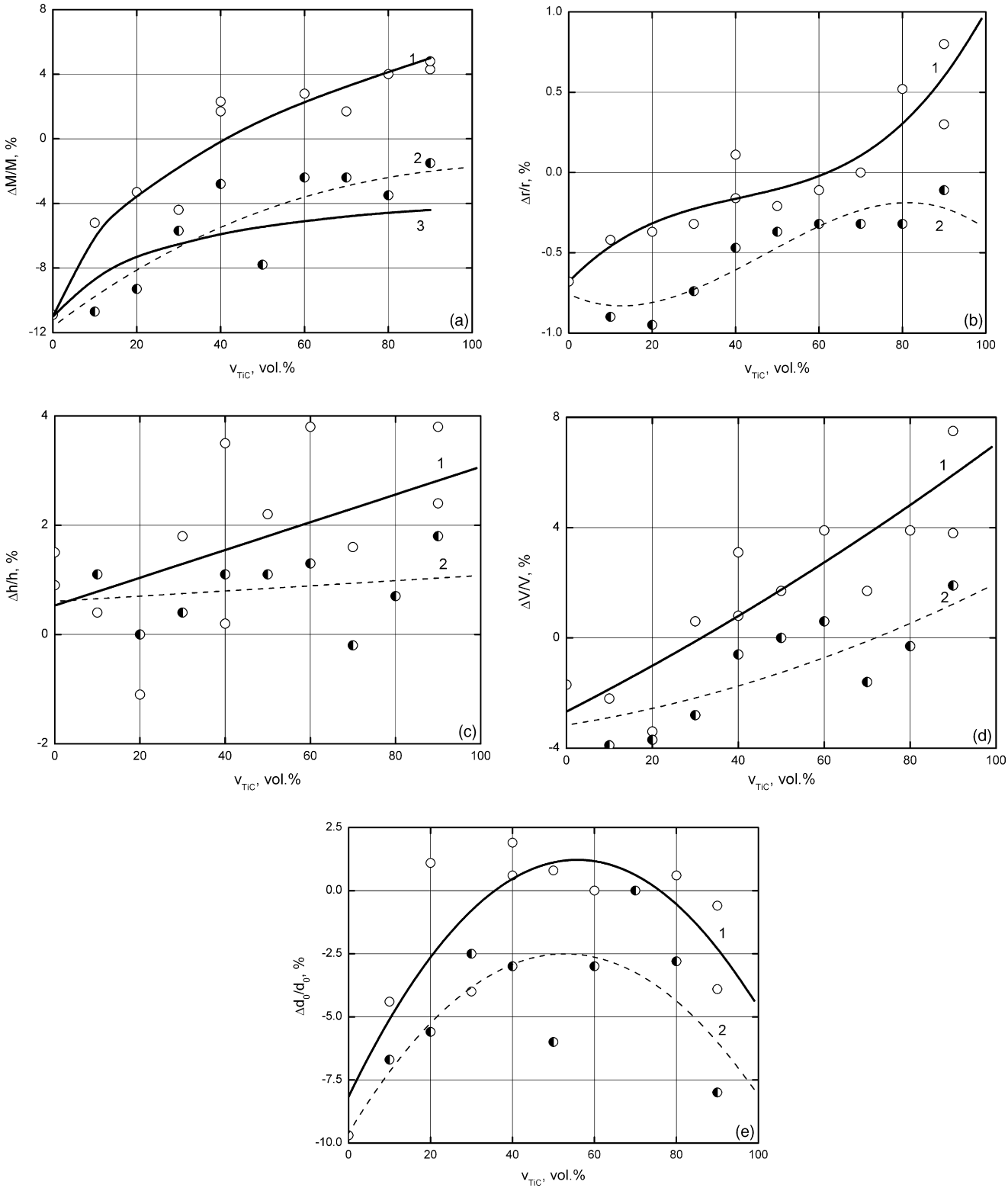

Fig. 8. The relative variation of mass (a), linear dimensions in radial (b) and coaxial (c) directions, volume (d) and apparent bulk density (e) vs. the volume content of carbide for the TiC–C (graphite) HMC with 30 vol% of Bakelite LBS-5 binder (1) in comparison with those for identically prepared and treated materials containing equimolar amounts of mixture $TiO_2 + 3C$ instead of TiC (2) (curve (3) in (a) is calculated using Eq. (11) for the $\Delta M/M$ plot).

1200 °C in protective CB layer. It was found that, for carbonisation with high heating rate and presence of metal carbide, this yield could be reduced to less than 35%. The TGA curves for the HMC with high and low carbide content significantly differ from each other. The oxidation of transition-metal monocarbide phases by the gaseous products of pyrolysis (H_2O, CO_2, CO), which starts at temperatures higher than 500 °C, leads the rich-carbide HMC to deviate significantly from the mass-loss values

observed during the carbonisation process for synthetic resins without any filler or with only the carbon filler present. The mechanism of the pyrolysis in the phenol–formaldehyde binder clearly changes in the presence of the carbide phase, essentially because water, which usually participates in the auto-oxidative mechanism of polymer carbonisation,[27] is involved in this case in the oxidation process of carbide phase of HMC. The transformation of carbide into oxide is accompanied by a significant increase of molar volume,[35] so oxide formation heightens the level of internal stresses in the carbonised carbide–carbon HMC. For several compositions, especially having been heat-treated at temperatures upward of 600 °C in vacuum, these stresses could lead to the partial rupture of the HMC. The modification of carbide–carbon HMC by refractory borides, which are more resistant to oxidation at 600–1000 °C, prevents this. An example of this was found with the 30 vol% ZrC–30 vol% ZrB_2–40 vol% C composition, where the carbonisation behaviour was more successful and similar to the graphite-rich materials (see Fig. 7a).

Unlike some of the other synthetic binders, phenol–formaldehyde resin is characterised by a significant shrinkage of the entire structure,[36] which approaches 50%. The pycnometric density–pyrolysis temperature plots for those resins[36–38] and some composites based on them,[39] in the wide temperature range from 200 to 1200 °C, are described by an S-shaped curve with low-temperature minimum at 400–500 °C, high-temperature maximum at 900–1100 °C and a quasi-linear part between the extremes. The linear shrinkage of Bakelite LBS-5 without any filler, during the treatment with heating rate of 5 °C min^{-1} in the range of 400–800 °C, effectively increases linearly with temperature.[40] However, in this temperature range, both apparent bulk and pycnometric densities of the carbonisation products also grow approximately linearly, leading to a constant level of porosity for the carbonaceous residue. The thermodestruction of pure LBS-5 occurs especially intensively at 500–530 °C. The structural transformation of 3D carbonaceous residue continues up to 850–950 °C. The resulting structure possesses a higher density compared with the 3D polycondensation structure of the initial polymer, as the yield of volatile products is not significant and the value of shrinkage is quite high. The propagation of decomposition by the formation of low-molecular-weight fragments allows the suborganic mass to conserve certain plasticity in the temperature range of intensive solid state pyrolysis. For the resin-bonded carbide–carbon HMC, whilst the carbonisation temperature increases, similar behaviour coupled with the high surface tension of carbonaceous residue and its significant adhesion to powder particle surfaces brings about the increase of volume shrinkage of the carbonised compacts, although in general the inherent weight loss of the material during the carbonisation process overmatches this shrinkage and results in a steady reduction of the bulk density (see Fig. 7b and c). The presence of catalysts, such as transition-metal carbides, probably lowers the plasticity due to an increase of the molecular weight of fragments[33] and elevates the porosity of carbonaceous residue because of an increase in volatile products yield,[16] so these circumstances hamper the preparation of the high-performance carbide-rich HMC. In spite of continuing liberation of gaseous pyrolysis products at temperatures higher than 650 °C, further increase of the heat treatment temperature does not lead to any noticeable reduction of the bulk density for the studied HMC.

The analysis of the relative variations of weight and dimensions for samples, which were heat-treated in an industrial electro-graphite carbonisation gaseous furnace, showed that these variations depend substantially on the carbide/carbon ratio in HMC. Fig. 8 represents the results of carbonisation heat treatment for the TiC–graphite HMC in comparison with identically prepared and treated compositions containing equimolar amount of $TiO_2 + 3C$ mixture instead of TiC. In spite of the intensive evolution of volatile products, which brings about a weight loss of material, the HMC with carbide content more than 40 vol% were characterised after carbonisation by an increase in weight, i.e. positive values of $\Delta M/M$. According to Eq. (11), and taking into account the experimentally obtained value of coke yield for the applied resin, the calculations were carried out for the $\Delta M/M$–v_{TiC} plot (Fig. 8a). It was found that the magnitudes of mass variation calculated from Eq. (11) are in better agreement with those for the samples containing the mixture of oxide with carbon than for compacts containing the carbide–carbon HMC. The deviation of calculated magnitudes from experimental data depends on the carbide content in HMC and can be explained via the oxidation processes of the carbide phase. The propagation of oxidation reactions was confirmed by XRD analysis of the carbonised samples of HMC. The results of this XRD analysis for the samples, which differed in carbide content and conditions of carbonisation, are summarized in Table 3. It is quite obvious that the interactions between carbides and products of pyrolysis reactions occur with some transformations of the carbide phases, including the formation of metal oxides. This was typical for carbonisation in vacuum, as well as for treatment under atmospheric pressure, and was independent of the rate of gas exchange for a wide range of temperatures and heating rates, so there is strong justification in suggesting an internal oxidation mechanism during the carbonisation process of HMC. Furthermore, microscopy, XRD phase analysis and EMPA for the external and internal areas of the cross-sections of the carbonised compacts provide solid grounds to remove the lack of uniformity of the samples from consideration and to confirm a predominant interaction of the carbide with H_2O, CO and CO_2, which are released from the degrading polymer.

The thermodynamic calculations carried out by Boosz[41] and Voitovich[42] for the reactions of transition-metal carbides with CO, CO_2 and H_2O showed that, not only are these reactions in the range of the temperatures from 400 to 1200 °C possible, but are preferable to those reactions of gasification of carbon by CO_2 and/or conversion of H_2O by carbon. In connection with this, Eq. (11) should be altered as follows:

$$\left(\frac{\Delta M}{M}\right)_{\kappa,\alpha} = \frac{K(100 - v_b)v_{MeC}d_{MeC}(\alpha/100) - cv_b d'_b(100 - \kappa)}{(100 - v_b)\left(v_{MeC}d_{MeC} + v_C d_C + \sum_{i=1}^{i=n} v_i d_i\right) + 100cv_b d'_b} \times 100\% \quad (13)$$

Table 3
Contents and structural characteristics of carbonised metal carbide–graphite HMC

Composition	Carbonisation parameters				Phases contents after carbonisation[a]	Lattice parameter of carbide phase[b] (nm)	
	Atmosphere	Heating rate (°C min^{-1})	Temperature (°C)	Treatment time (h)		Before carbonisation	After carbonisation
10 vol% TiC–90 vol% C	10–100 Pa, pyrolysis products	∼100	400–600	2	C, TiC_xO_y	0.4328 ± 0.0003	0.431 ± 0.001
			700–900		C, TiC_xO_y, TiO_2(r)[c]		0.430 ± 0.004
90 vol% TiC–10 vol% C			400–500		TiC_xO_y, C		0.4305 ± 0.0008
			600–700		TiC_xO_y, TiO_2(r + a)[d], C		0.430 ± 0.002
			800–900		TiC_xO_y, TiO_2(r), C		0.429 ± 0.003
10 vol% TiC–90 vol% C	∼100 kPa, atmosphere of combustion products in gas furnace	<0.5	1200	200	C, TiC_xO_z, TiO_2(r)	0.4328 ± 0.0003	0.426 ± 0.005
30 vol% TiC–70 vol% C					C, TiC_xO_z, TiO_2(r)		0.427 ± 0.005
50 vol% TiC–50 vol% C					TiC_xO_z, TiO_2(r), C		0.425 ± 0.004
60 vol% TiC–40 vol% C					TiC_xO_z, TiO_2(r), C		0.424 ± 0.006
70 vol% TiC–30 vol% C					TiC_xO_z, TiO_2(r), C		0.424 ± 0.004
80 vol% TiC–20 vol% C					TiC_xO_z, TiO_2(r), C		0.422 ± 0.005
90 vol% TiC–10 vol% C					TiC_xO_z, TiO_2(r), C		0.423 ± 0.004
10 vol% ZrC–90 vol%C	10–100 Pa, pyrolysis products	100	400–500	2	C, ZrC_xO_y	0.4695 ± 0.0003	0.4665 ± 0.0006
			600–800		C, ZrC_xO_y, ZrO_2(t)[e]		0.454 ± 0.003
90 vol% ZrC–10 vol% C			400–500		ZrC_xO_y, C		0.4622 ± 0.0008
			600		ZrC_xO_y, ZrO_2(c)[f], C		0.460 ± 0.002
			700		ZrC_xO_y, ZrO_2(c + t)[g], C		0.451 ± 0.003
			800		ZrO_2(t), ZrC_xO_y, C		0.446 ± 0.006
30 vol% ZrC–30 vol% ZrB_2–40 vol% C			400–500		ZrC_xO_y, ZrB_2, C		0.466 ± 0.002
			600–700		ZrC_xO_y, ZrB_2, ZrO_2(t + m)[h], C		0.455 ± 0.003
			800		ZrB_2, ZrO_2(t + m), ZrC_xO_y, C		0.455 ± 0.005

[a] Results of XRD analysis.
[b] Dispersion was calculated at 95% confidence level.
[c] r, rutile modification of TiO_2.
[d] r + a, mixture of rutile and anatase modifications of TiO_2.
[e] t, tetragonal modification of ZrO_2.
[f] c + t, mixture of cubic and tetragonal modifications of ZrO_2.
[g] c, cubic modification of ZrO_2.
[h] t + m, mixture of tetragonal and monoclinic modifications of ZrO_2.

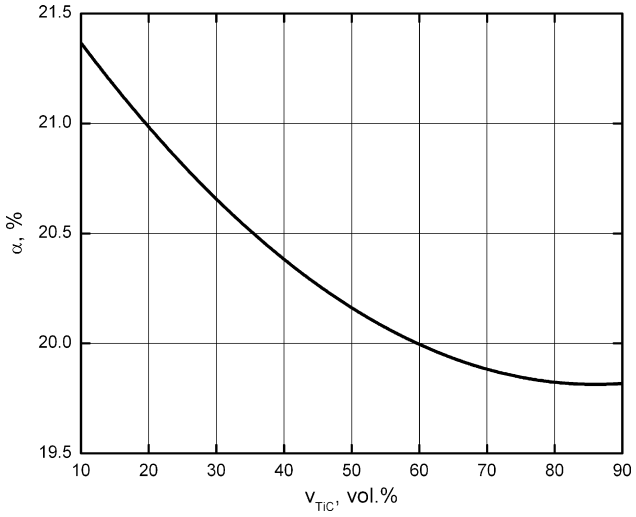

Fig. 9. The rate of interaction between carbide phase and products of pyrolysis α vs. the volume content of carbide for the TiC–C (graphite) HMC with 30 vol% of Bakelite LBS-5 binder calculated using Eq. (13).

where K is the stoichiometric coefficient for these systems ($K = 0.534$, 0.310 and 0.168 for TiC, ZrC and HfC, respectively) and α is the rate of interaction between the carbide phase and the products of pyrolysis (%). This equation is in good agreement with experimental dependencies of the relative variations of mass for the synthetic resin-bonded carbide–carbon HMC obtained after carbonisation. The rate of interaction α, represents a gross-characteristic of the carbide–oxide transformation during the carbonisation process. The calculated values of α, according to experimental data (Fig. 8a) and Eq. (13), are shown in Fig. 9 as a function of carbide content for the HMC containing TiC. The increase of α with the reduction of carbide content in the materials also confirms the internal nature of the carbide oxidation process and its spread throughout the bulk of the HMC compacts.

This method of comparative analysis of carbonisation behaviour for materials containing carbide and oxide also allows the assessment of the contribution of the oxidation process of the carbide to the variation of linear and volume dimensions of carbonised carbide–graphite compacts. The partial transformation of carbide to oxide leads to an increase of both radial and coaxial dimensions of the compact, so volume shrinkage is observed only for materials with carbide content less than 30 vol%, which demonstrates a weak contribution of the oxide formation process to the volume variation. It was also revealed that the carbonised carbide–graphite HMC have a tendency to swell by as much as 5%. The mass increase of such carbonised compacts due to oxidation has a compensatory influence on the apparent bulk density, so for the TiC–C HMC in the range of carbide contents from 20 to 80 vol%, the apparent bulk density does not change significantly after carbonisation. However, the carbonisation is very sensitive to the carbide and oxide content because of the influence of these compounds on the polymerisation and pyrolysis processes, which are themselves dependant on the physico-chemical nature of the filler. Deviations of the $\Delta M/M$–content plot for carbonised compacts containing oxide from the values, calculated according to Eq. (11) for inert filler, confirmed the specific influence of oxide on the physico-chemical transformation of binder and its properties during the curing and subsequent heat treatment of these materials. The introduction of interaction rate α for the description of carbonisation process should be considered to be an attempt to approximate the interaction between carbide phases and pyrolysis products, because the real process of carbide oxidation involves the formation of other, more complicated phases such as oxycarbides MeC_xO_y (see Table 3). The XRD patterns for carbonised carbide–graphite HMC are characterised by significant variations in profile and position of the diffraction peaks, for which carbonised samples had lower intensities and higher values of half-width. This results in a significant increase of statistical dispersion for the determined values of carbide phase lattice parameters.

Thus, the presence of the synthetic binder, such as phenol–formaldehyde resin, in the carbide–carbon HMC changes the process of formation of these structures due to the mutual influence of the fine powder composition and the organic binder. The experimental data obtained in the present work demonstrates the high degree of chemical interaction between the carbide components of HMC and the thermally-degrading polymer; a situation requiring improved heat-treatment procedures in order to fabricate high-performance carbide-rich HMC.

3.3. Thermal shock/fatigue resistance testing

The main purpose of thermal shock resistance testing was to compare the performance of carbide–graphite HMC, obtained in this work by the carbonisation of synthetic resin-bonded compacts, with those of high-temperature heat-treated materials with the same carbide content. Hence two types of HMC were tested for the degradation of their strength characteristics during thermal shock cycling: a composition hot-pressed from powder at 2700 °C and 12 MPa, 70 vol% TiC–30 vol% C (TKU-3)[6] and the composition with the same carbide/graphite ratio bonded by 30 vol% of Bakelite LBS-5 and carbonised by heating up to 1200 °C with a working cycle of 200 h in a multi-chamber gaseous electro-graphite carbonisation furnace (see Table 2). The determined values of the tensile rupture strength for compositions that underwent different thermal loading were quoted to the ultimate tensile strength at room temperature for TKU-3 (σ_0) and plotted in coordinates σ/σ_0–N (number of thermal shock cycles). The resulting curves for both materials are shown in Fig. 10. Possessing lower tensile strength, the synthetic resin-bonded materials nevertheless appeared to be more successful in thermal shock/fatigue resistance than the composition with higher strength characteristics and this was due to the specific structure of the material formed during the interaction between the powder composition and the carbonised binder. A detailed justification of this conclusion will require additional investigation and is beyond the scope of this work. For further optimisation of the microstructure of synthetic resin-bonded carbide–graphite HMC, with an eye to improving desirable physical properties, a thorough study of the transformations in the materials during the heat treatment processing is required

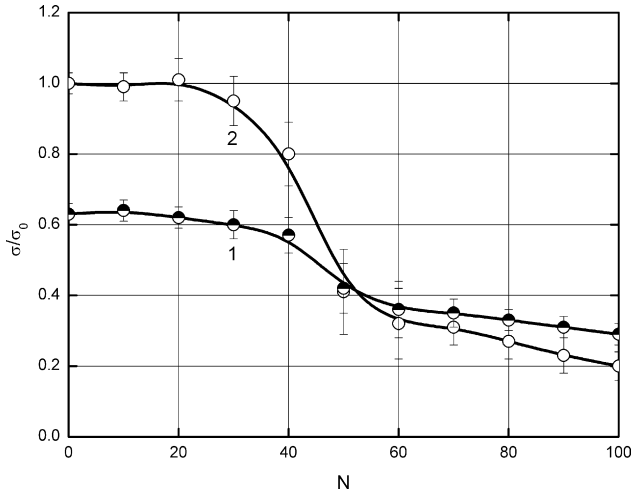

Fig. 10. The normalised tensile strength vs. number of thermal shock cycles for the 70 vol% TiC–30 vol% C (graphite) HMC: (1) cured-pressed and carbonised with 30 vol% of Bakelite LBS-5; (2) high-temperature hot-pressed.

to produce a generic process for consistent manufacture of this type of ceramic.

4. Conclusions

This work has essentially been a novel, process-orientated study of the transition-metal carbide–graphite compositions with synthetic binder for the fabrication of HMC. The process included a precursory curing-pressing procedure as well as carbonisation heat treatment, which was accompanied by the dual processes of pyrolysis of the binder and carbide oxidation. In summary:

1. A mathematical model for the properties of carbide–carbon compacts with synthetic binder was developed employing the statistical fractional factorial experimental design with a 2^{5-2} matrix type for a number of processing parameters. Applying fundamental principles of powder technology, the model was extended over primarily studied factorial space to interpret the specific behaviour of compositions with a synthetic binder. The pressing procedure was characterised by a viscous flow of binder into the intergranular spaces of the powder composition. This flow was accompanied by the polycondensation process of the resin, which was affected by catalytic properties of the solid surfaces of transition-metal carbide particles.
2. The processes of pyrolysis of the polymer binder began at rather lower temperatures than was observed for the phenol resin without any filler and confirmed the influence of transition-metal carbides as catalysts of similar reactions. Though the experimentally determined value of the coke yield for Bakelite LBS-5 amounted to $50.5 \pm 0.5\%$, it could be reduced by 35% or more due to the cumulative effect of high rates of heating and the presence of metal carbide. However, a back influence of the binder was also detected, in particular, pyrolysis products on the carbide. The rate of interaction between these products and the carbide phase after carbonisation for a 200 h cycle with maximum temperature of 1200 °C exceeded the value of 20% complete transformation of carbide and led to the partial oxidation with the formation of complicated intermediate phases, such as oxycarbides MeC_xO_y, as well as metal oxides. Therefore, the behaviour of carbide–graphite HMC during the carbonisation process was shown to depend strongly on the carbide content in these materials. The compensational influence of the mass increase inherent for the carbonised compacts, due to carbide oxidation, resulted in the invariance in the apparent bulk density after the carbonisation process for the TiC–C HMC in the range of carbide contents from 20 to 80 vol%.
3. Possessing lower tensile strength when compared with high-temperature hot-pressed materials, the synthetic resin-bonded HMC nevertheless possess better thermal shock/fatigue resistance characteristics.

Acknowledgements

One of the authors, I.L. Shabalin wishes to thank Prof. A.R. Beketov, Ural State Technical University, Russia, for providing the necessary technological and research facilities and both authors would like to express their gratitude to Prof. D.K. Ross for support and assistance in the preparation this work for publication.

References

1. Kendall, E. G., Carnahan, R. D. and Rossi, R. C., Hypereutectic carbides highly resistant to thermal shock. *Space/Aeronautics*, 1967, **47**(1), 132–133, 135.
2. Harada, Y., High strength hot-pressed metal carbide–graphite composites. *Report NASA–CR–77114*, IIT Research Inst., Chicago, IL, 1966.
3. Hasselman, D. P. H., Becher, P. F. and Mazdiyasni, K. S., Analysis of the resistance of high-*E*, low-*E* brittle composites to failure by thermal shock. *Z. Werkstofftech.*, 1980, **11**(3), 82–92.
4. Zhukov, Yu. N., Cherepanov, A. V., Beketov, A. R. and Shabalin, I. L., Inspection of the nonuniformity of a ceramic compact for machining by hardness measurement. *Sov. Powder Metall. Met. Ceram.*, 1991, **30**(4), 349–351.
5. Shabalin, I. L., Beketov, A. R., Gorinskii, S. G., Podkovyrkin, M. I. and Fedorenko, O. V., Study of strength characteristics of titanium carbide–silicon carbide–carbon hot-pressed materials. In *Alloys of Refractory and Rare Metals for High-Temperature Application. Proceedings of the All-USSR Conference on Physico-Chemical Principles of Development for Heat-Resisting Metal Materials*, ed. E. M. Savitskii. Nauka, Moscow, 1984, pp. 186–189.
6. Gorinskii, S. G., Shabalin, I. L., Korshunov, I. G., Beketov, A. R. and Kokorin, A. F., Thermophysical properties of hot-pressed TiC–C and ZrC–C composite materials at high temperatures. *Sov. Powder Metall. Met. Ceram.*, 1979, **18**(4), 266–269.
7. Pakholkov, V. V., Gorinskii, S. G., Beketov, A. R., Shabalin, I. L. and Ragozin, S. V., Texture of the hot-pressed vanadium carbide–carbon materials. *Sov. Powder Metall. Met. Ceram.*, 1986, **25**(8), 661–663.
8. Tong, Q., Shi, J., Song, Y., Guo, Q. and Liu, L., Resistance to ablation of pitch-derived ZrC/C composites. *Carbon*, 2004, **42**(12–13), 2495–2500.
9. Araki, M., Sasaki, M., Kim, S., Suzuki, S., Nakamura, K. and Akiba, M., Thermal response experiments of SiC/C and TiC/C functionally gradient materials as plasma facing materials for fusion application. *J. Nucl. Mater.*, 1994, **212–215**, 1329–1334.
10. Shabalin, I. L., Beketov, A. R., Vlasov, V. G. and Pakholkov, V. V., Towards a question of carbide–carbon composite manufacturing by hot-pressing. In

Hot-pressing, *Vol. 2*, ed. M. S. Kovalchenko. Ukrainian SSR Academy of Science Institute for Problems of Materials Science, Kiev, 1977, pp. 15–18.
11. Beketov, A. R., Shabalin, I. L. and Fedorenko, O. V., Hot-pressed and fused carbide–carbon materials. *Tsvetn. Met.*, 1979, **3**, 39–42.
12. Inagaki, M., Research and development carbon/ceramic composites in Japan. *Carbon*, 1991, **29**(3), 287–295.
13. Ewais, E. M. M., Carbon based refractories. *J. Ceram. Soc. Jpn.*, 2004, **112**(10), 517–532.
14. Suvorov, S. A., Denisov, D. E., Timofeev, V. F., Kuznetsov, G. I., Kortel, A. A., Kuznetsov, Yu. D. *et al.*, Phenol-furfural binder for refractories. *Refractories*, 1993, **34**(11), 559–560.
15. Suvorov, S. A., Denisov, D. E. and Vanicheva, L. L., Reaction of phenol–formaldehyde bond with refractory filler. *Refractories*, 1986, **27**(7–8), 454–459.
16. Denisov, D. E., Epstein, S. M., Karyavin, A. A. and Suvorov, S. A., Carbonization of a phenol–formaldehyde binder based on a periclase filler. *Refractories*, 1989, **30**(3–4), 195–199.
17. Uzberg, L. V., Sizov, V. I., Malyutin, A. A., Myakisheva, N. A. and Prudnikova, N. N., Properties of periclase materials produced using carbonaceous binders. *Refractories*, 1986, **27**(9–10), 559–562.
18. Lemon, P. H. R. B., Phenol formaldehyde polymers for the bonding of refractories. *Trans. J. Br. Ceram.*, 1985, **84**(2), 53–56.
19. Funabiki, K., Nakamura, M. and Tsuriya, M., Phenolic resin and its application for refractories. *Taikabutsu*, 1981, **33**(2), 64–80.
20. Dubois, J., Fantozzi, G., Bougoin, M. and Thevenot, F., Microstructure et properietes mecaniques de materiaux ceramiques de type B_xC/SiC frittes sans charge. *J. Phys. Paris Colloq.*, 1986, **47**(2), 751–755.
21. Rabinovich, A. S., Kazakov, S. V. and Vanicheva, L. L., Optimization of the composition and the properties of the plastic bodies for obtaining silicon carbide products. *Refractories*, 1993, **34**(3–4), 188–192.
22. Beketov, D. A., Beketov, A. R. and Khoroshavin, L. B., Composite coatings based on aluminium nitride and an organic binder. *Refractories*, 2003, **44**(1), 65–66.
23. Afonin, Yu. D., Shalaginov, V. N. and Beketov, A. R., Communications interface for the Elektronika DZ-28 microcomputer and experimental equipment. *Instrum. Exp. Tech.*, 1984, **27**(6/1), 1374–1377.
24. Krasnov, A. N., Zilberberg, V. G. and Sharivker, S. Yu., *Low-Temperature Plasma in Metallurgy*. Metallurgiya, Moscow, 1970, pp. 44–49.
25. Sedokov, L. M. and Sampilov, Ts. D., Determination of tensile strength from tests of ceramic bushings in radial compression. *Strength Mater.*, 1982, **14**(4), 426–431.
26. Balshin, M. Yu., *Powder Metallurgy*. Metallurgizdat, Moscow, 1948, pp. 40–52.
27. Ouchi, K., Infra-red study of structural changes during the pyrolysis of a phenol–formaldehyde resin. *Carbon*, 1966, **4**, 59–66.
28. Fitzer, E. and Schafer, W., The effect of cross-linking on the formation of glasslike carbons from thermosetting resins. *Carbon*, 1970, **8**, 353–364.
29. Yamashita, Y. and Ouchi, K., A study on carbonization of phenol–formaldehyde resin labeled with deuterium and ^{13}C. *Carbon*, 1981, **19**, 89–94.
30. Lum, R., Wilkins, C. W., Robbins, M., Lyons, A. M. and Jones, R. P., Thermal analysis of graphite and carbon–phenolic composites by pyrolysis-mass spectrometry. *Carbon*, 1983, **21**(2), 111–116.
31. Morterra, C. and Low, M. J. D., I.R. studies of carbons—VII. The pyrolysis of a phenol–formaldehyde resin. *Carbon*, 1985, **23**(5), 525–530.
32. Lausevic, Z. and Marinkovic, S., Mechanical properties and chemistry of carbonization of phenol formaldehyde resin. *Carbon*, 1986, **24**(5), 575–580.
33. Lukina, Ye. Yu., Demin, A. V., Kosinski, K. A. and Rakcheeva, V. I., The effect of refractory elements and their compounds on the character of thermal processes during carbonization and properties of obtained carbon materials. In *Proceedings of All-USSR Meeting on Solid State Chemistry*, ed. G. P. Shveikin. Ural Division of the USSR Academy of Sciences Institute of Chemistry, Sverdlovsk–Pervouralsk, 1975, pp. 44–45.
34. Dollimore, D. and Heal, G. R., The degradation of selected polymers to carbons in an inert atmosphere. *Carbon*, 1967, **5**, 65–72.
35. Kuptsov, S. G., Vlasov, V. G., Beketov, A. R., Shabalin, I. L., Fedorenko, O. V. and Pykhteev, Yu. P., The low-temperature oxidation mechanism of zirconium carbide. In *Kinetics and Mechanism of Reactions in Solid State*, ed. E. A. Prodan. Byelorussian State University, Minsk, 1975, pp. 182–183.
36. Marcovic, V. and Marinkovic, S., A study of pyrolysis of phenolic resin reinforced with carbon fibres and oxidized PAN fibres. *Carbon*, 1980, **18**, 329–335.
37. Ko, T. H., The effect of pyrolysis on the mechanical properties and microstructure of carbon fiber-reinforced and stabilized fiber-reinforced phenolic resins for carbon/carbon composites. *Polym. Compos.*, 1993, **14**(3), 247–256.
38. Ko, T. H., Kuo, W. S. and Chang, Y. H., Microstructural changes of phenolic resin during pyrolysis. *J. Appl. Polym. Sci.*, 2000, **81**, 1084–1089.
39. Manocha, L. M., Bhatt, H. and Manocha, S. M., Development of carbon/carbon composites by co-carbonization of phenolic resin and oxidized PAN fibers. *Carbon*, 1996, **34**(7), 841–849.
40. Samsonov, B. A., Butyugin, V. K. and Sigarev, A. M., A study of features for variation of the density of carbonization products for several polymers. In *Structural Materials Based on Carbon*, *Vol. 9*, ed. V. I. Kostikov. Metallurghiya, Moscow, 1974, pp. 190–200.
41. Boosz, H. J., Die bestandigkeit von hartstoffen gase. *Metall*, 1956, **10**(3/4), 130–136.
42. Voitovich, R. F., *Refractory Compounds. Thermodynamic Characteristics*. Naukova Dumka, Kiev, 1971, pp. 30–42.